Himawari-9
Navigation and Calibration

1. Image navigation and registration
2. Radiometric calibration

JMA/MSC Data Processing Department
Application and Analysis Division
22 November 2022

1. Image navigation and registration

Image navigation and registration

Displacement based on landmark analysis relating to coastlines

B07

B13

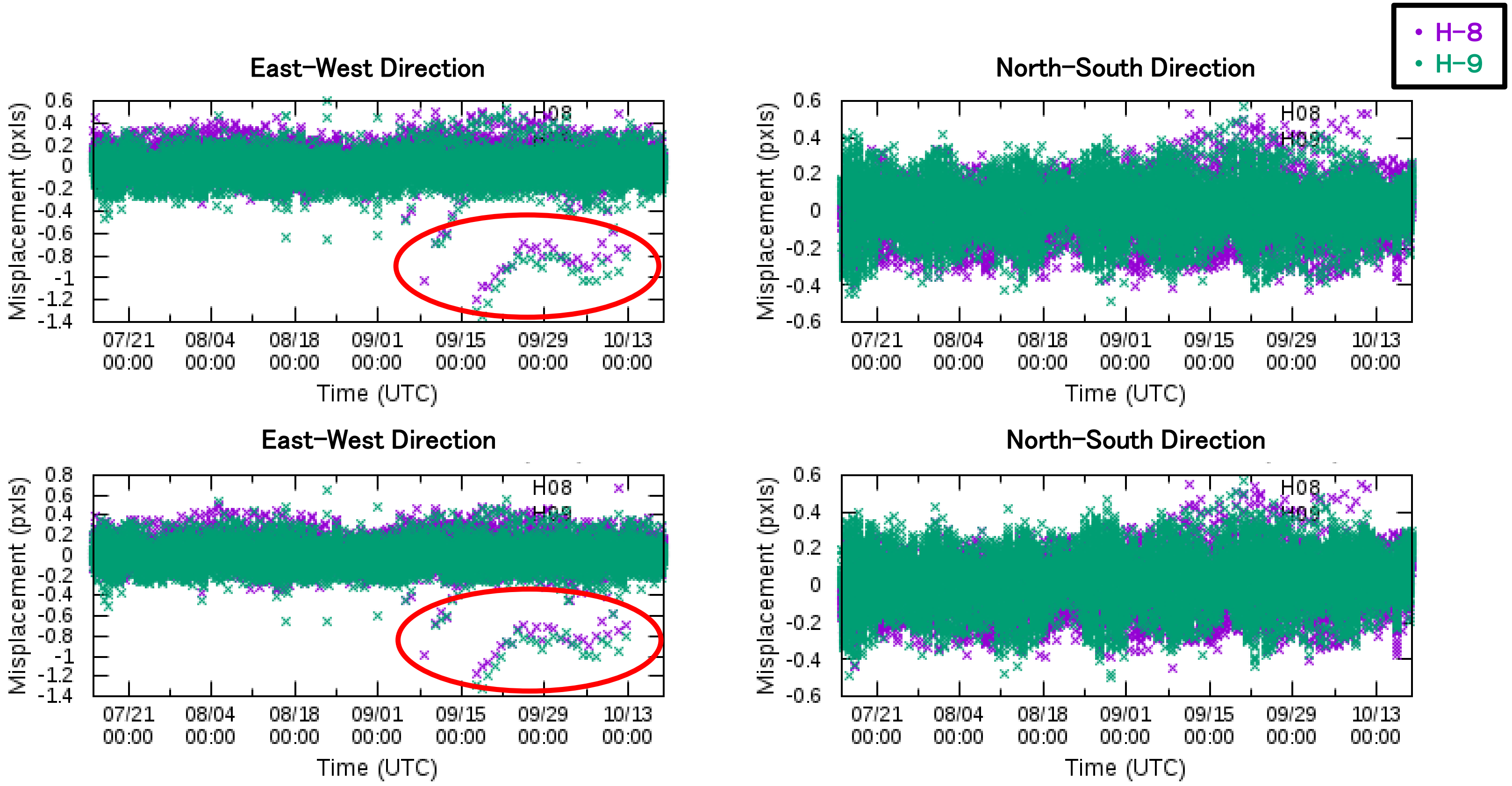

- While some fluctuations are observed, displacement is similar for Himawari-8 (H-8) and Himawari-9 (H-9) in each band.
- The red circle shows midnight data in an eclipse season.
- The trend of H-9 is similar to that of H-8, including the presence of outliers.
- Partial image loss caused by sun avoidance is not included in the evaluation.

※ 1pixel corresponds to 2km.

Image navigation and registration

Band to Band registration with reference to Band 13

30th July 2022 Daily average Band to Band Registration (BBR) Error.

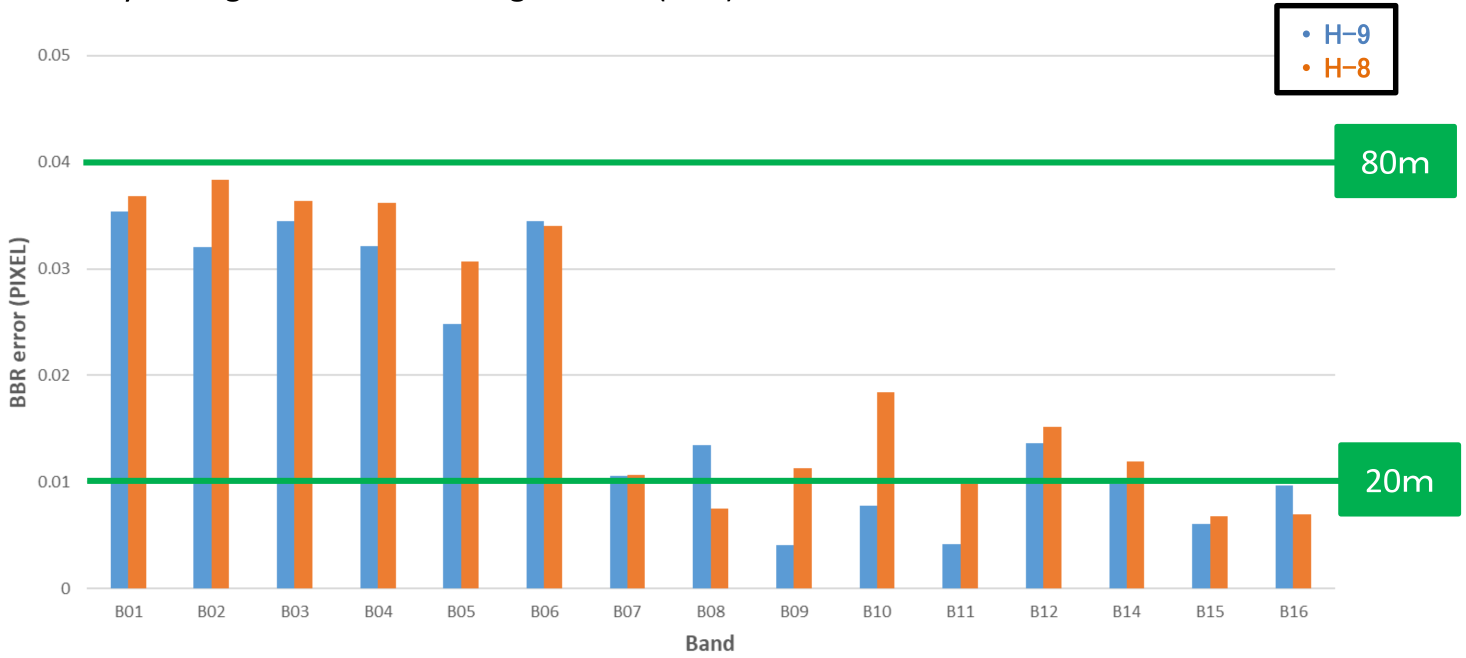

※ 1pixel corresponds to 2km.

Although minor error differences are observed in some bands, H-9 accuracy is comparable to that of H-8.

Image navigation and registration

Band to Band registration with reference to Band 13

The minor BBR error compared to the error on 30th July (shown on the previous slide) originates from annual fluctuation.

18th Oct 2022 Daily average Band to Band Registration (BBR) Error.

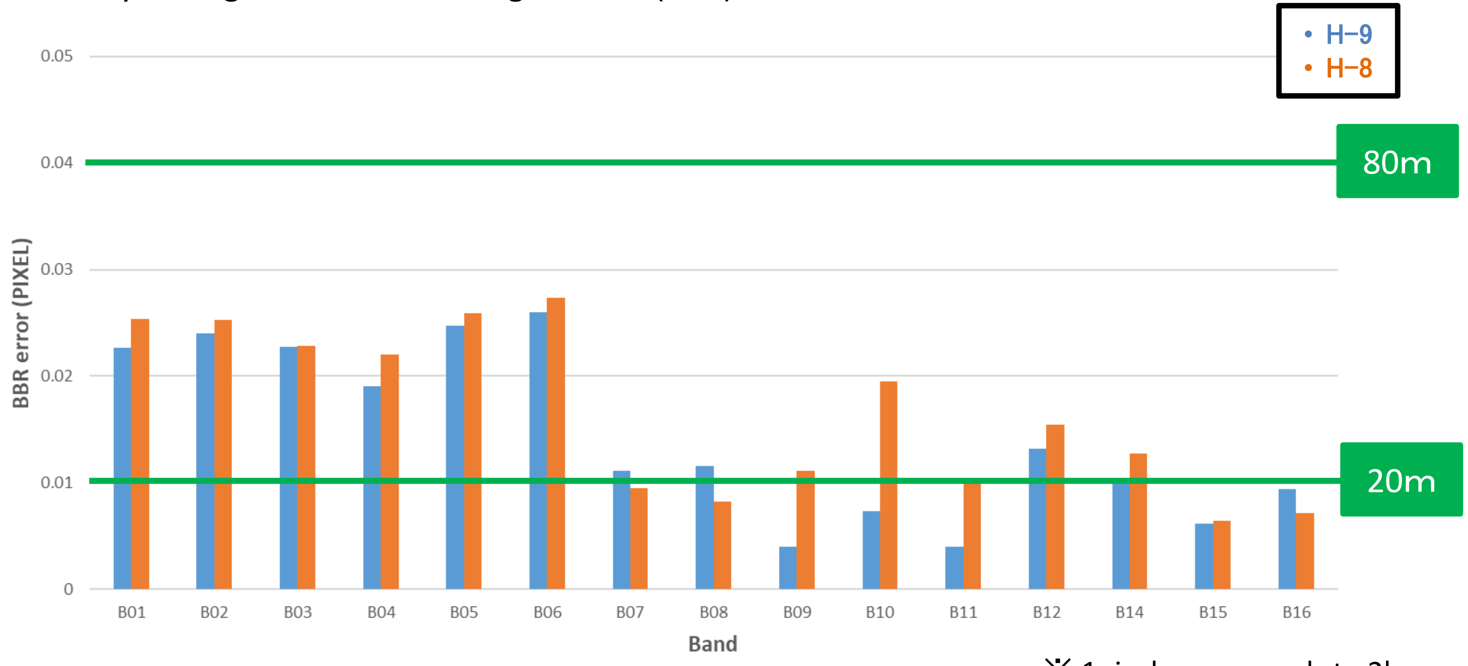

※ 1pixel corresponds to 2km.

Although minor error differences are observed in some bands, H-9 accuracy is comparable to that of H-8.

Image navigation and registration

Band to Band registration with reference to Band 13

B01

The gradual decrease in displacement is attributed to annual fluctuations.

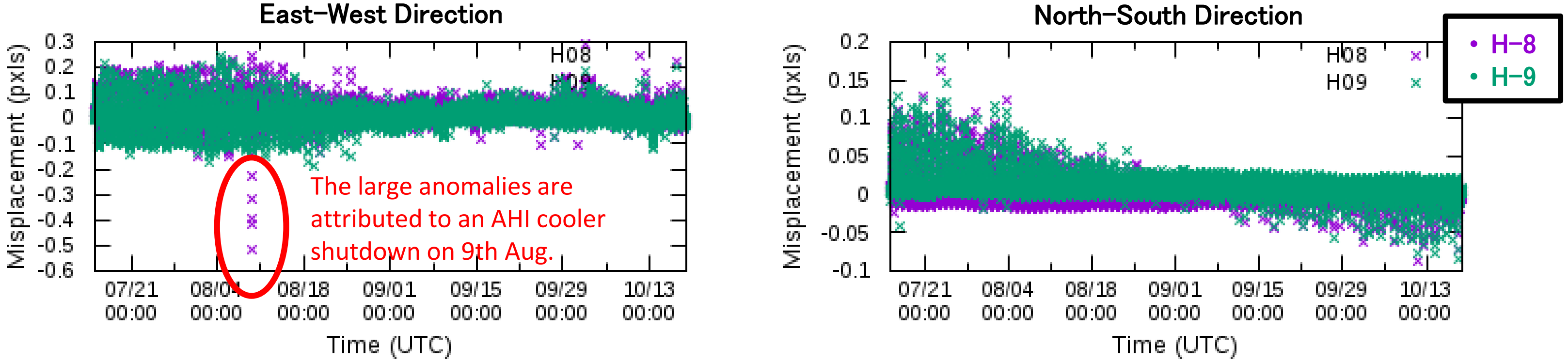

B02

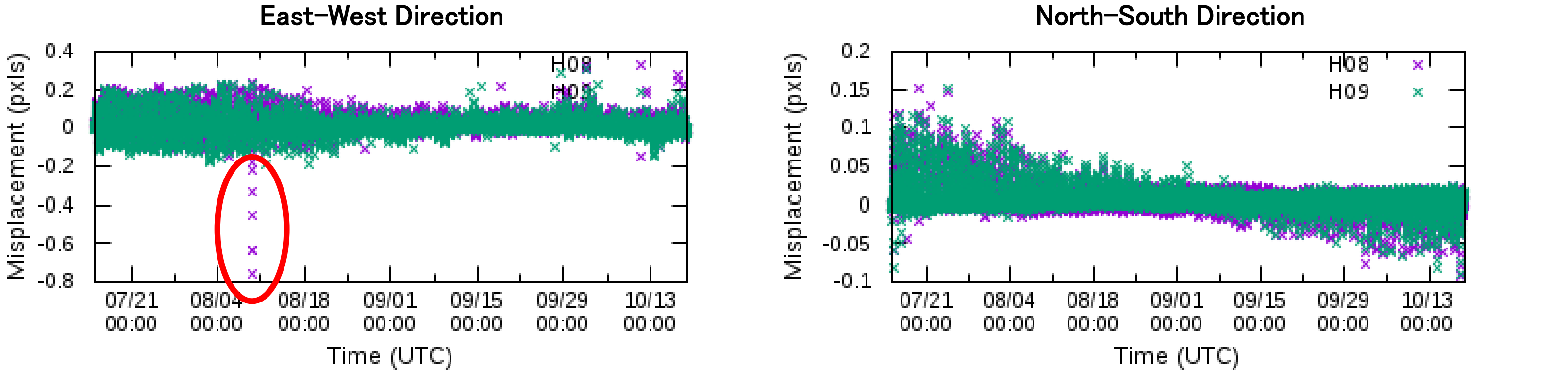

B03

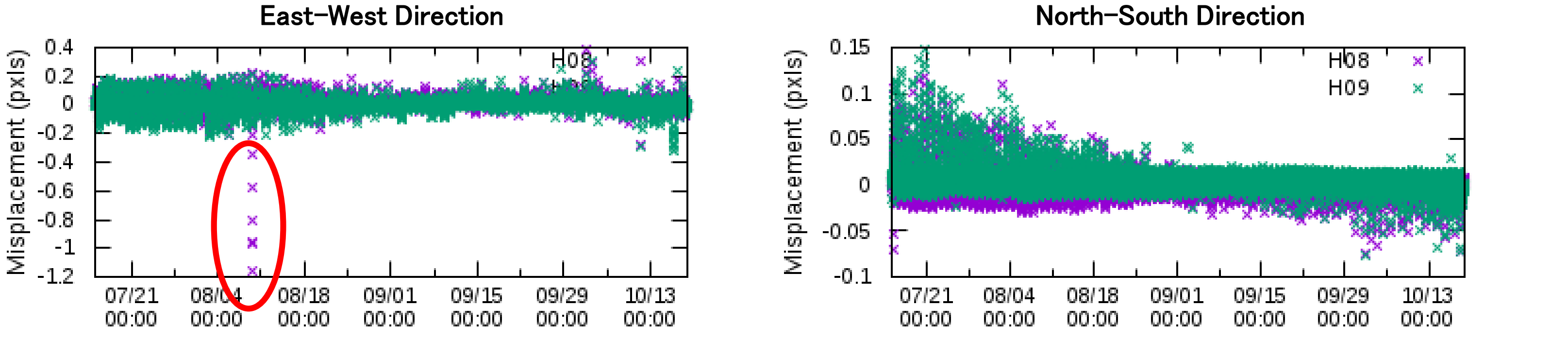

※ 1pixel corresponds to 2km.

Image navigation and registration

Band to Band registration with reference to Band 13

B04

The gradual decrease in the amount of displacement is due to annual fluctuations.

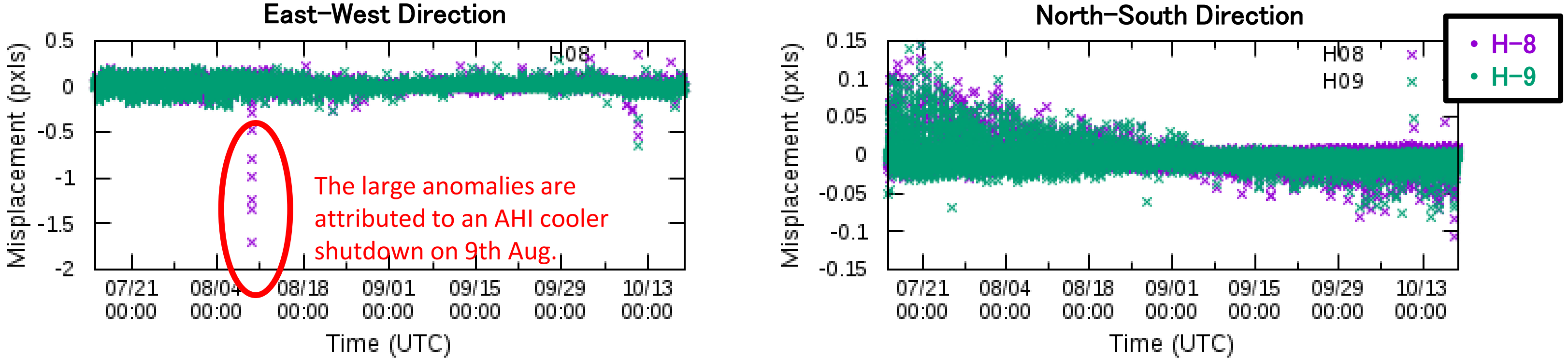

B05

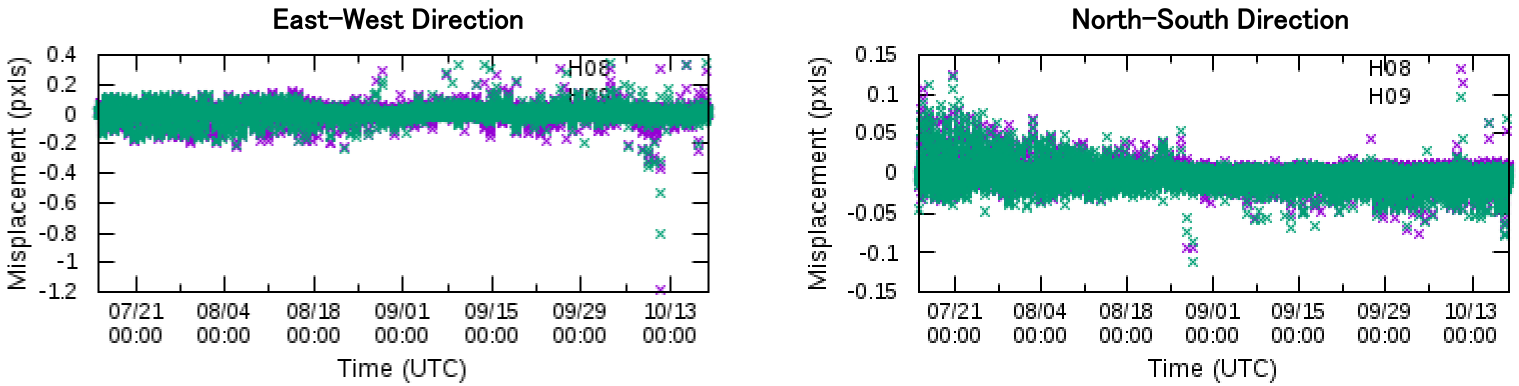

B06

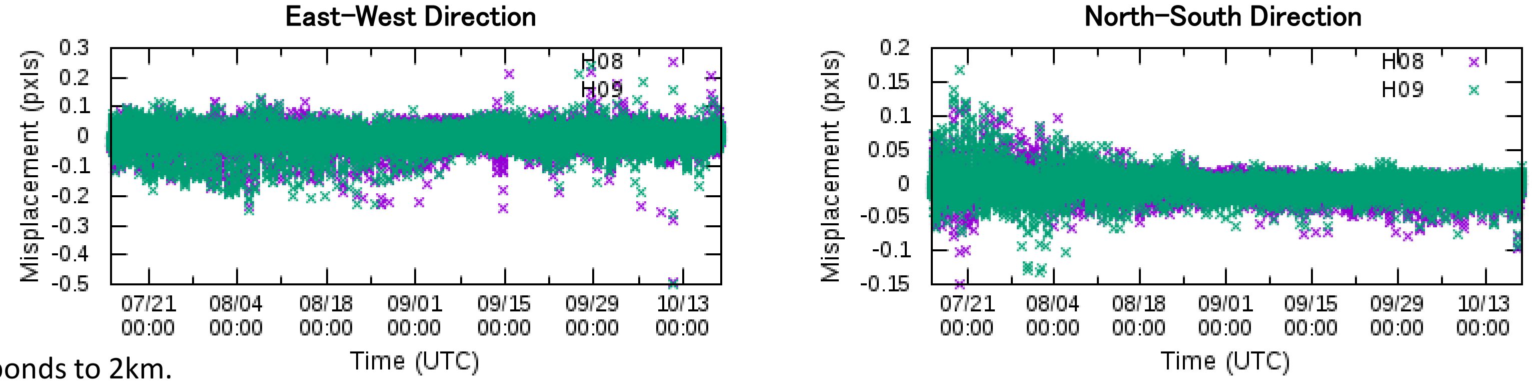

※ 1pixel corresponds to 2km.

Image navigation and registration

Band to Band registration with reference to Band 13

B07

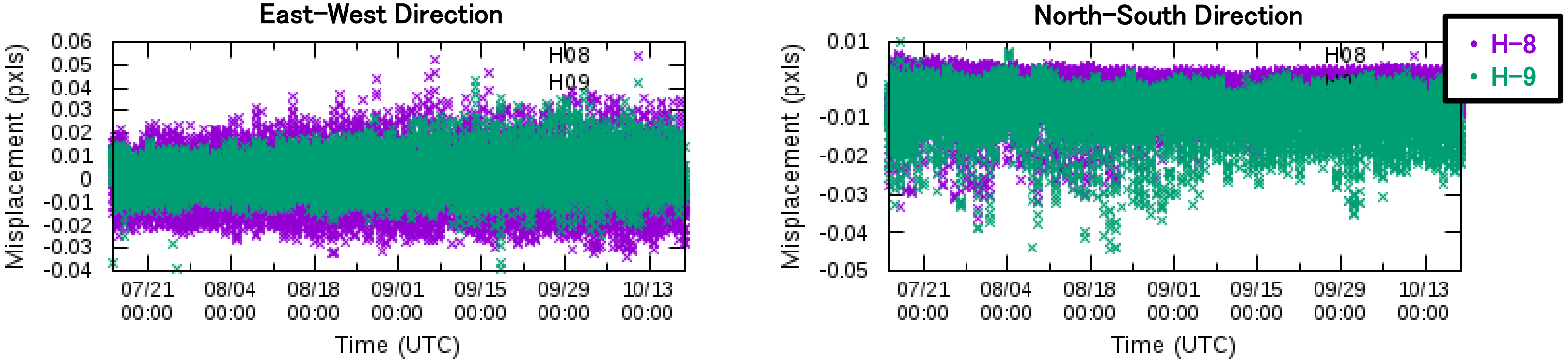

B08

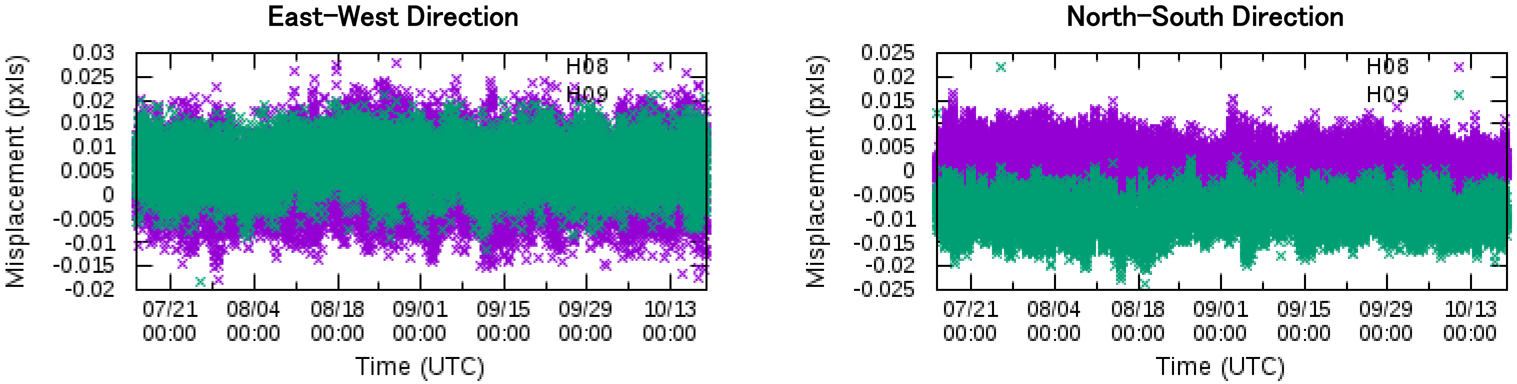

B09

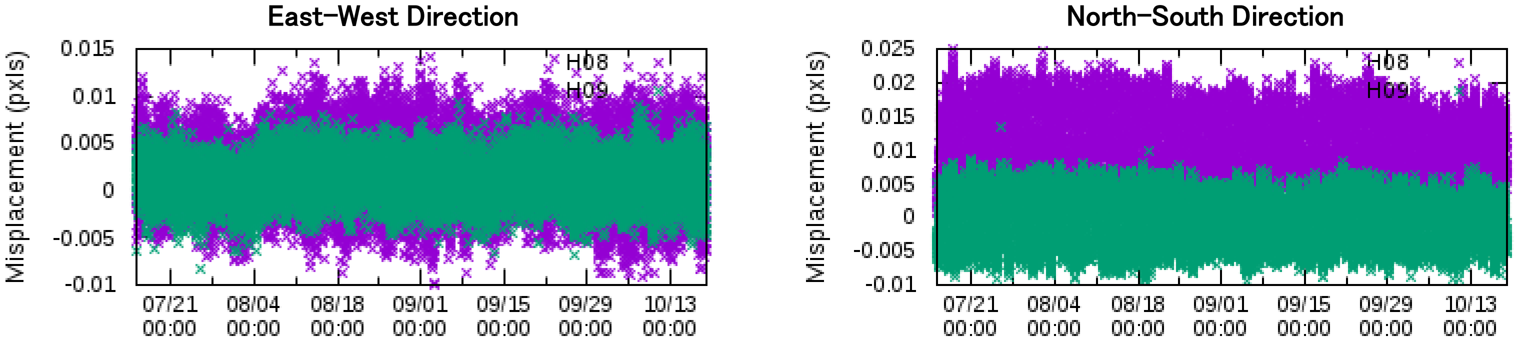

※ 1pixel corresponds to 2km.

Image navigation and registration

Band to Band registration with reference to Band 13

B10

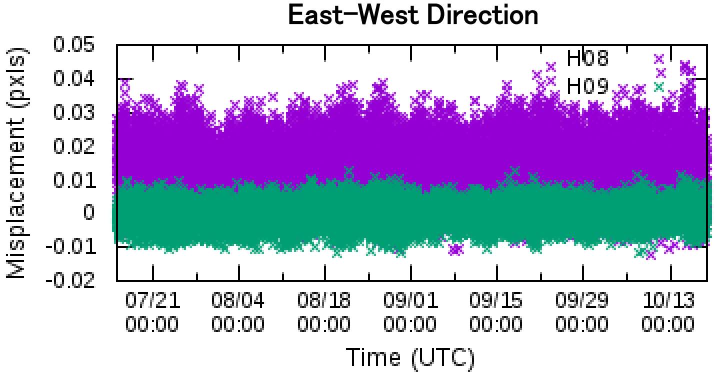

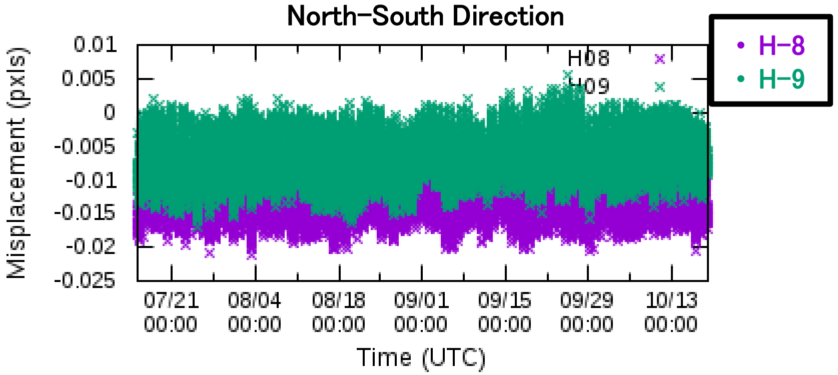

B11

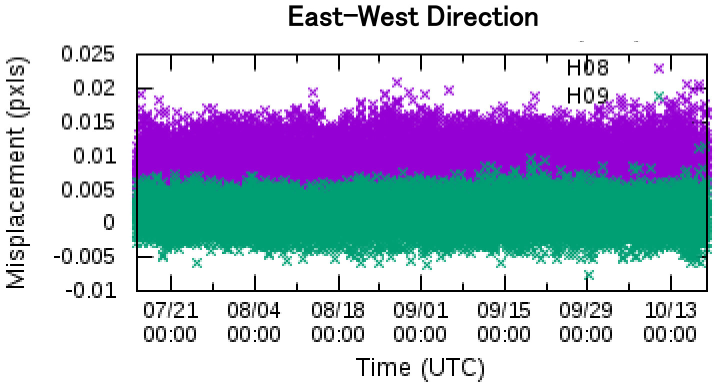

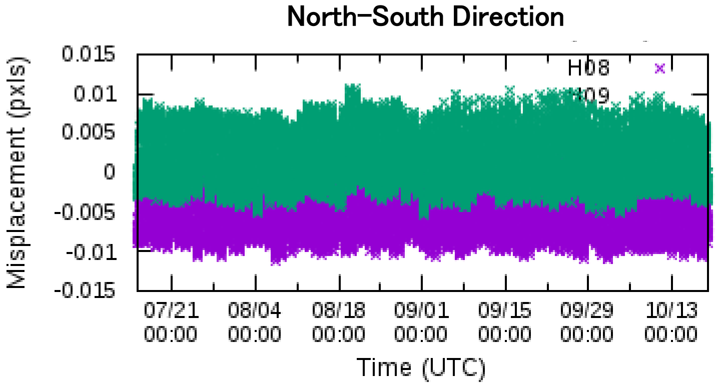

B12

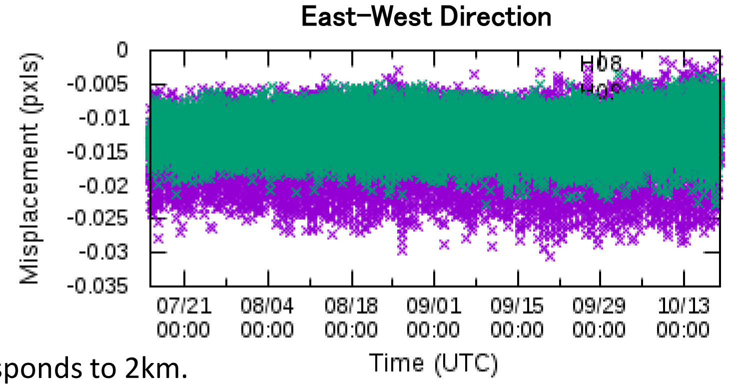

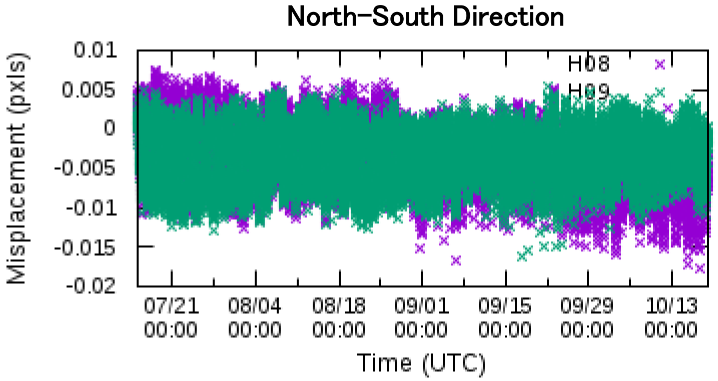

※ 1pixel corresponds to 2km.

Image navigation and registration

Band to Band registration with reference to Band 13

B14

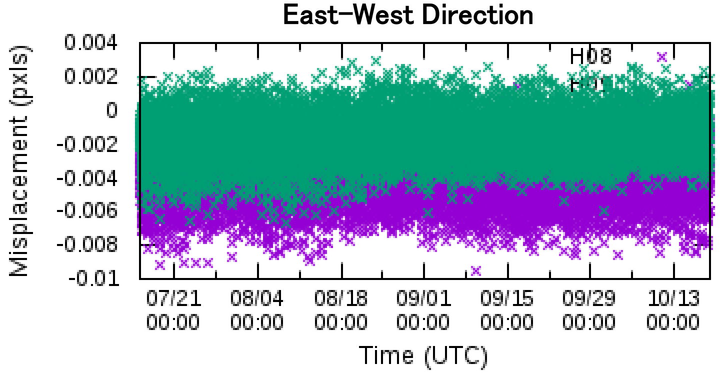

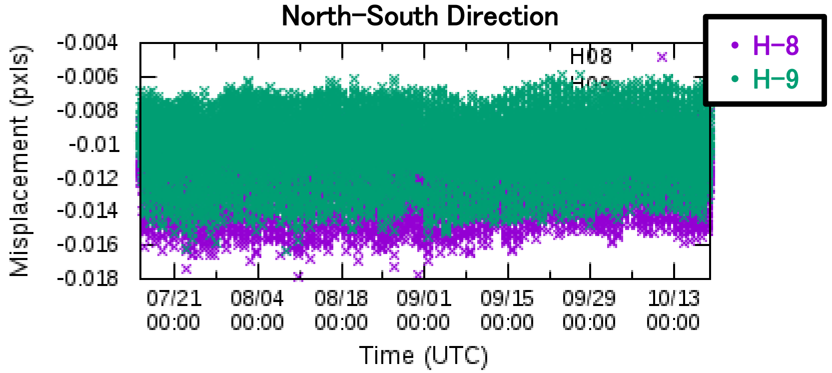

B15

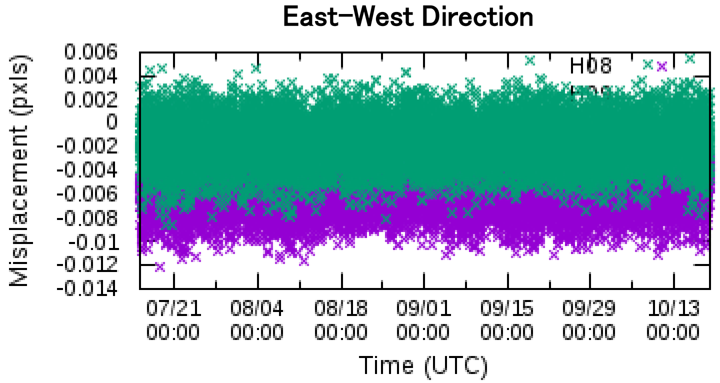

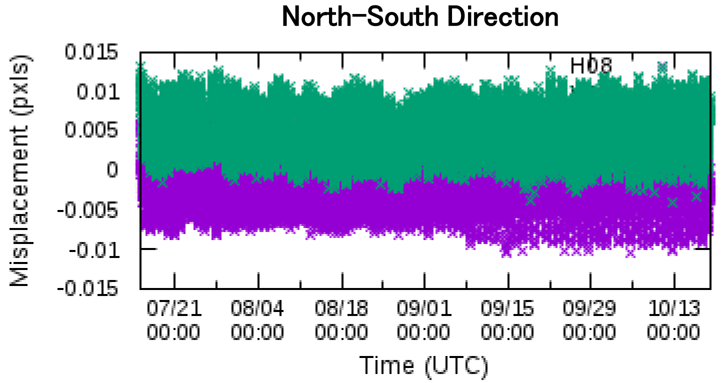

B16

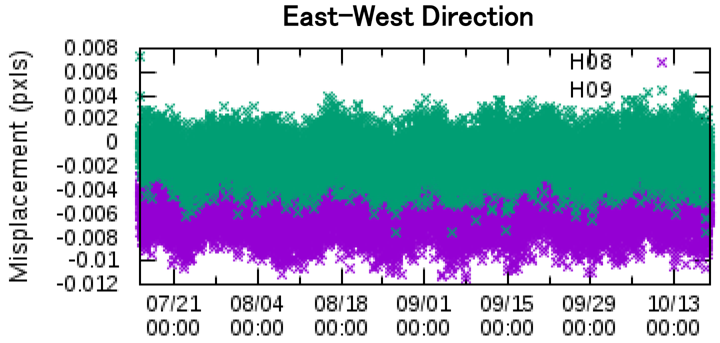

Time (UTC)

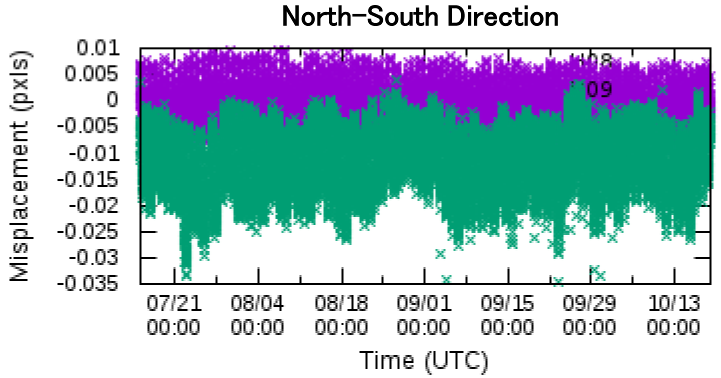

※ 1pixel corresponds to 2km.

2. Radiometric Calibration

Evaluation of calibration

I. Direct comparison between H-8 and H-9

- Results
  - Results show simple comparison of observations from both satellites.
  - Results do not match exactly due to sensor differences.
- Application

  By way of example, the results can support evaluation of H-9 L2 products retrieved using H-8 parameters.

II. Evaluation of calibration in consideration of SRF differences (e.g., GSICS)

- Results
  - Results show remaining biases in consideration of observation discrepancies caused by SRF differences between AHIs.
- Application?

  By way of example, the results can support evaluation of H-9 L2 products retrieved using H-9 parameters.

The example of SRFs measured on the ground test.

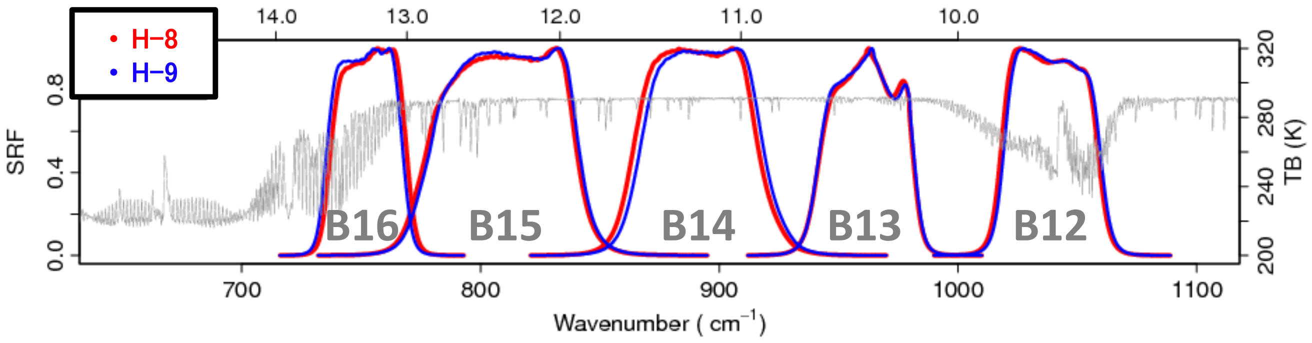

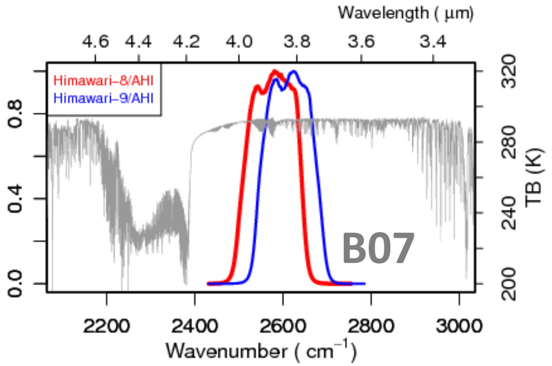

I. Direct comparison of H-8 and H-9

- Differences in observed reflectivity (H-9 minus H-8)
- Percentage discrepancies caused by SRF differences

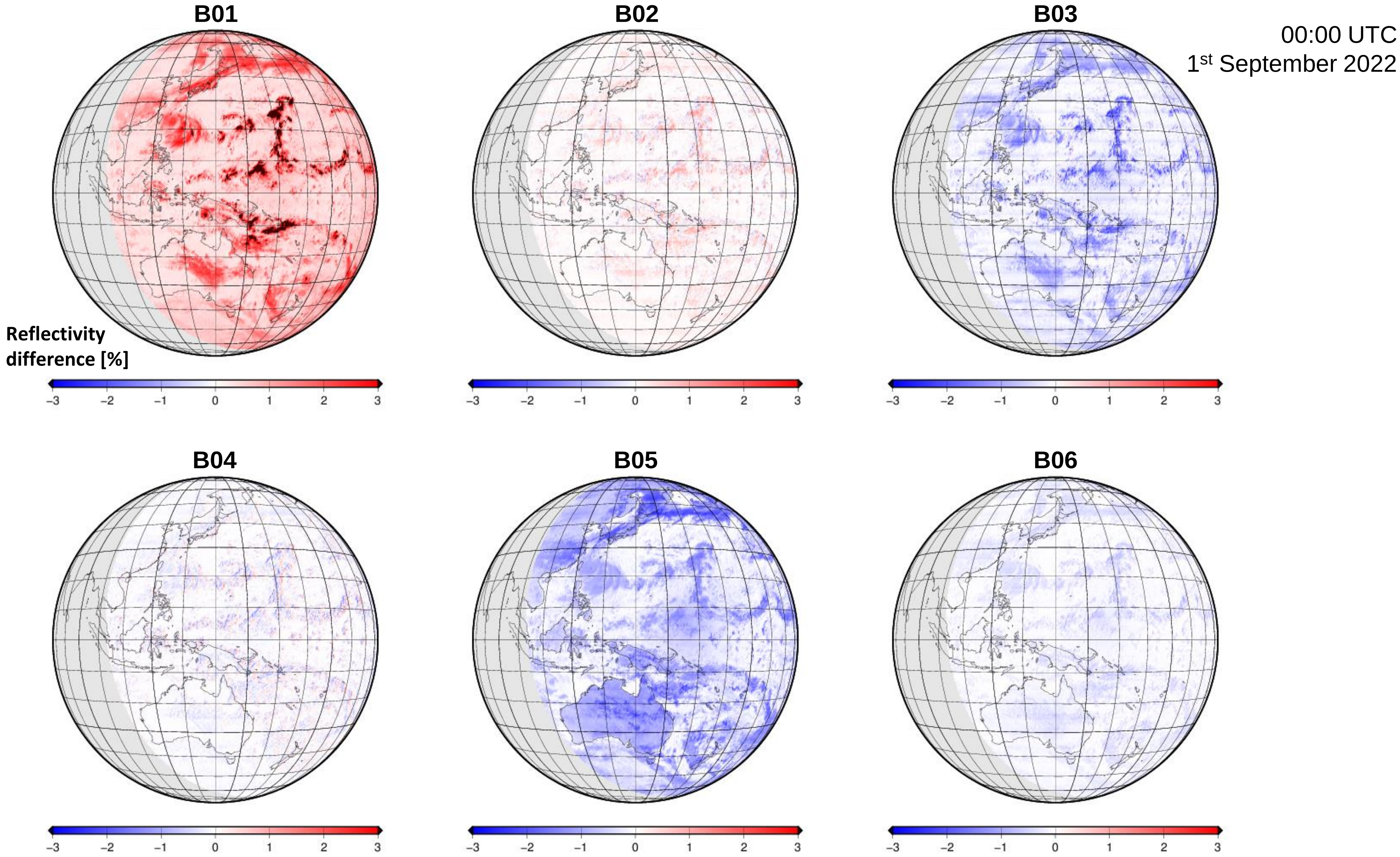

I. Direct comparison of H-8 and H-9

- Stable linear relationship since the start of H-9 observation in 2022

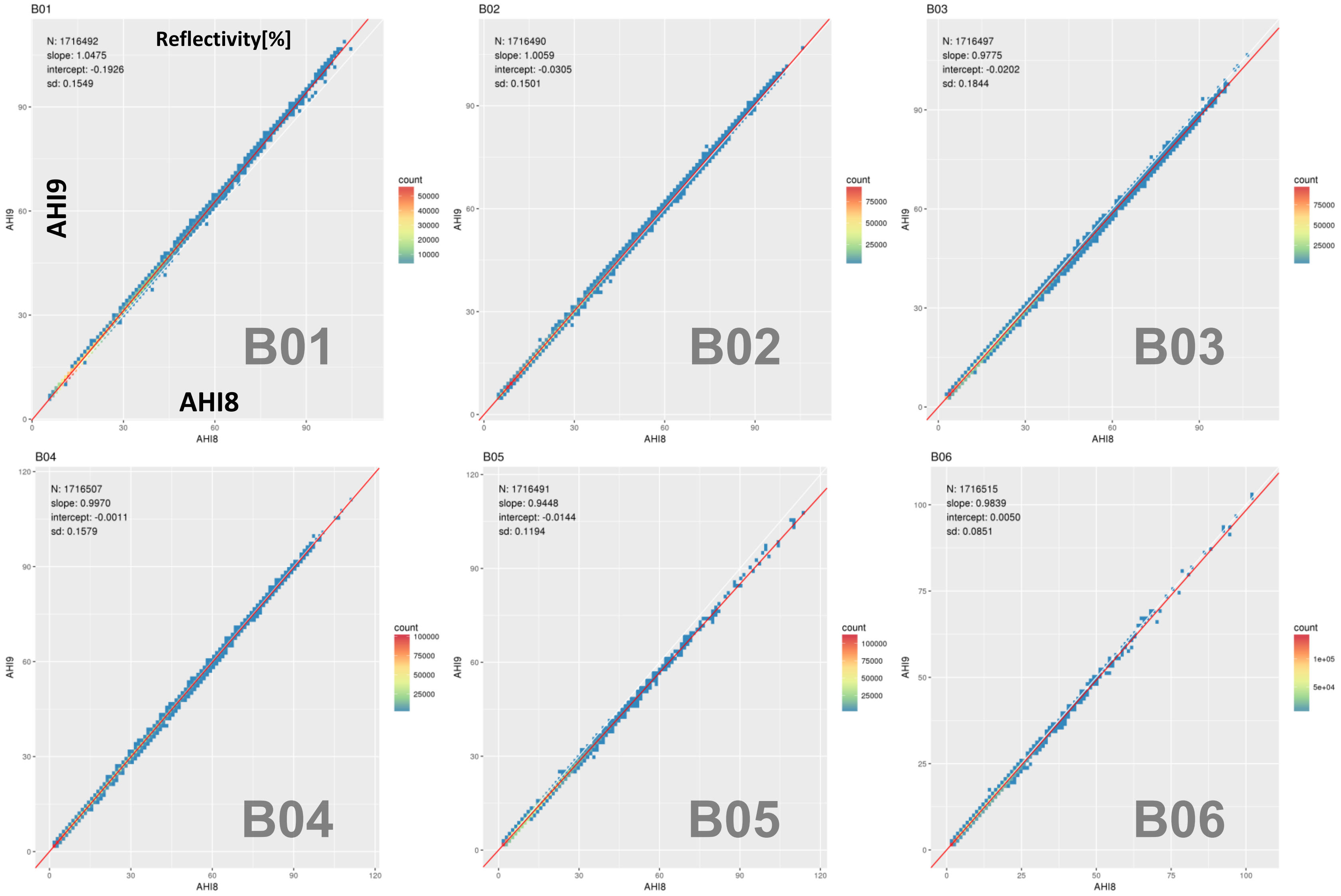

Data period:
1st - 7th October 2022

Conditions:
- 00 – 06 UTC (Daytime)
- Sun zenith angle: less than 70 deg.
- Data from outside the Earth disk not included

I. Direct comparison of H-8 and H-9

- Differences in brightness temperature (Tb) (H-9 minus H-8)
- Discrepancies caused by SRF differences

00:00 UTC
1st September 2022

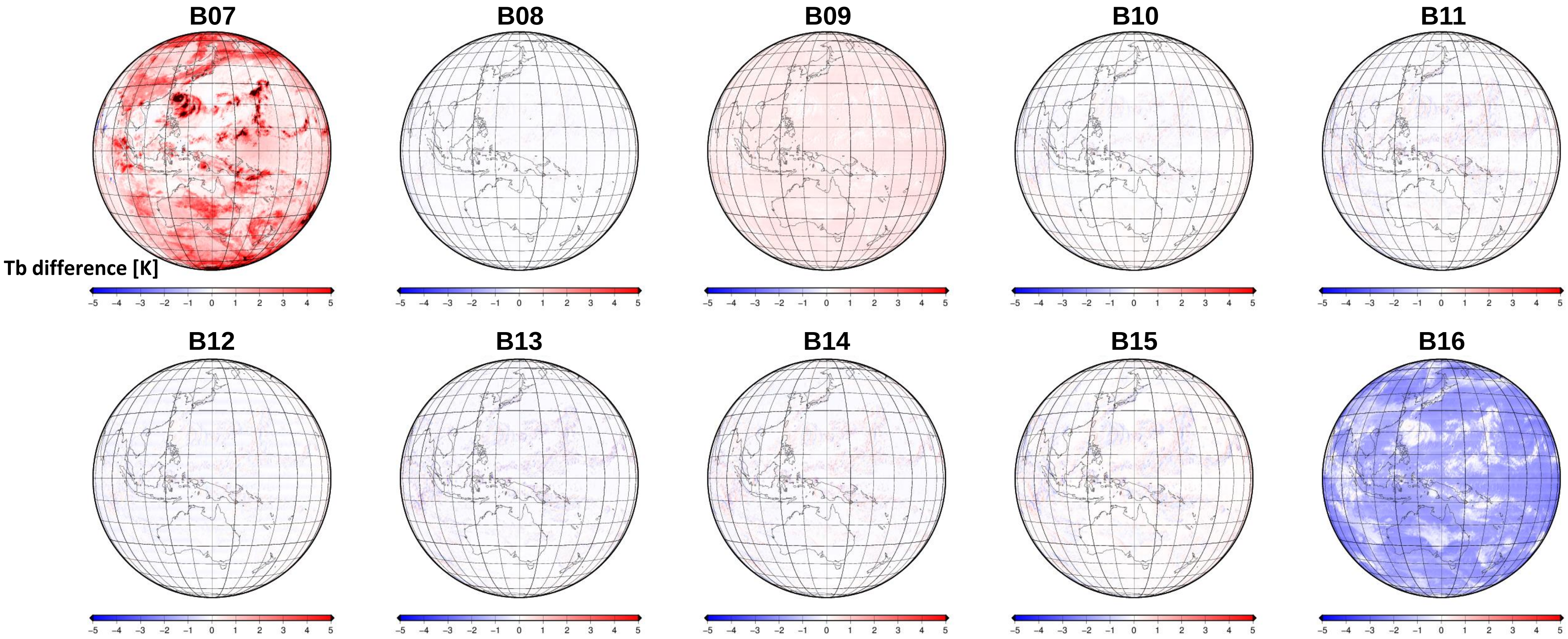

I. Direct comparison of H-8 and H-9

- Stable linear relationship since the start of H-9 observation in 2022

Data period:
1st - 7th October 2022
Conditions:
- 10 – 13 UTC (Nighttime)
- Sun zenith angle: larger than 110 deg.
- Data from outside the Earth disk not included

Brightness temperature [K]

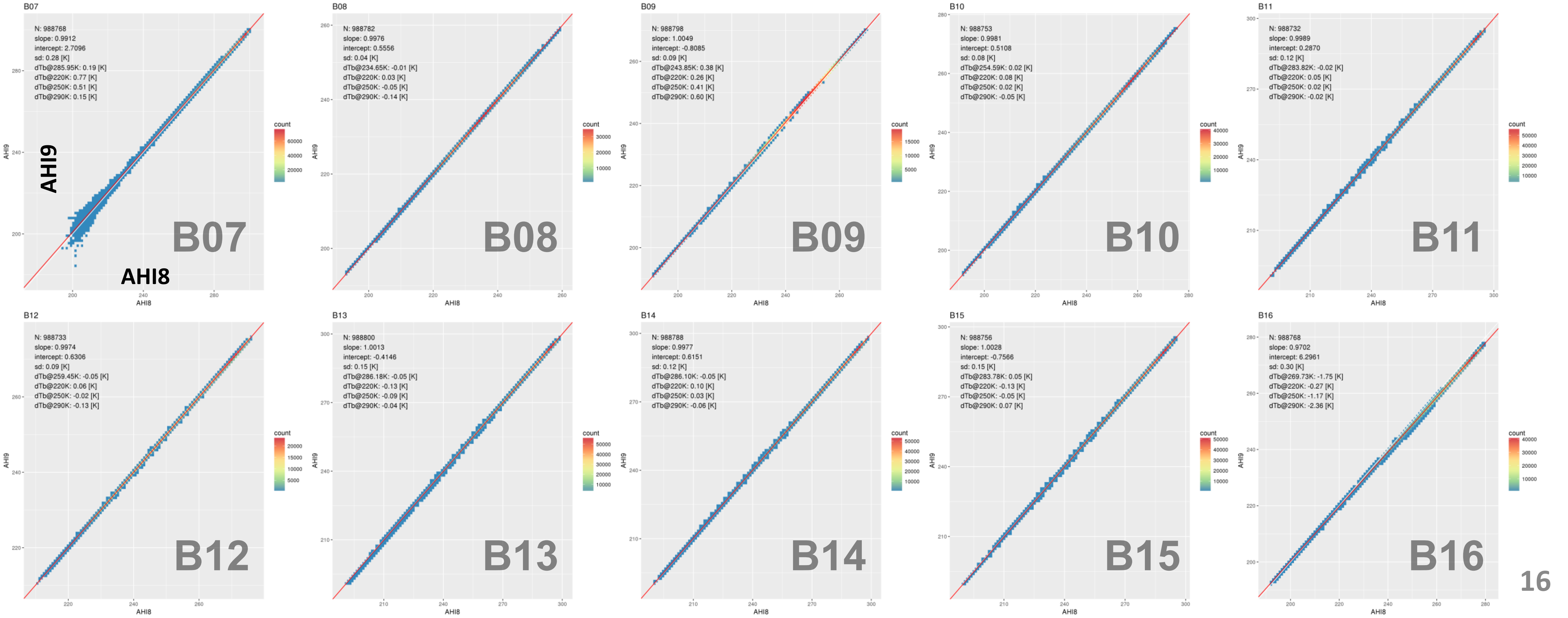

I. Direct comparison of H-8 and H-9

Linear regression coefficients

	Slope	Offset
B01	1.04750	-0.19260
B02	1.00594	-0.03052
B03	0.97746	-0.02018
B04	0.99698	-0.00105
B05	0.94478	-0.01444
B06	0.98394	0.00502

	Slope	Offset	H9-H8 [K] @StdTb.*	H9-H8 [K] @220K	H9-H8 [K] @250K	H9-H8 [K] @290K
B07	0.99118	2.70964	0.19 @285.95K	0.77	0.51	0.15
B08	0.99759	0.55558	-0.01 @234.65K	0.03	-0.05	-0.14
B09	1.00486	-0.80853	0.38 @243.85K	0.26	0.41	0.60
B10	0.99805	0.51075	0.02 @254.59K	0.08	0.02	-0.05
B11	0.99893	0.28697	-0.02 @283.82K	0.05	0.02	-0.02
B12	0.99738	0.63064	-0.05 @259.45K	0.06	-0.02	-0.13
B13	1.00129	-0.41459	-0.05 @286.18K	-0.13	-0.09	-0.04
B14	0.99766	0.6151	-0.05 @286.10K	0.10	0.03	-0.06
B15	1.00284	-0.75661	0.05 @283.78K	-0.13	-0.05	0.07
B16	0.97016	6.29606	-1.75 @269.73K	-0.27	-1.17	-2.36

* Std.Tb: Brightness temperature corresponding to clear-sky sea surface (band-dependent)

Data period: 1st – 7th October 2022, 00-06UTC (for B01-B06), 10-13UTC (forB07-B16)

Stability of linear regression coefficients

- Statistics from August to October 2022 show stable linear regression coefficients.

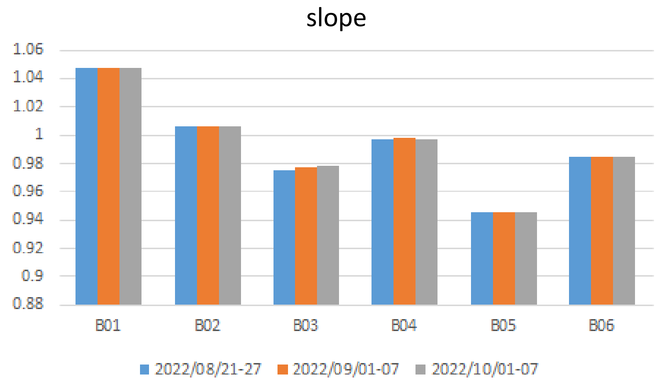

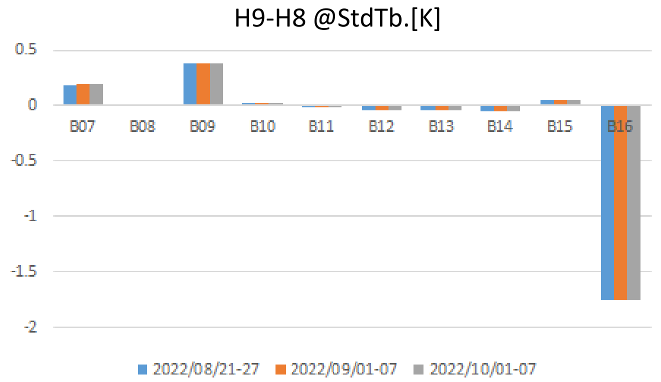

II. Evaluation of calibration in consideration of SRF differences (B01 – B06)

Approaches

- Two approaches are applied to evaluate calibration accuracy in consideration of SRF differences between H-9 and reference imagery.
- Ray-matching[1]: Here, H-9 observation data are compared with VIIRS data from SNPP and NOAA-20. SRF differences between AHI and VIIRS are considered using correction coefficients (SBAF[2]) based on ENVISAT/SCIAMACHY data.
- RTM based (vicarious calibration) approach[3]: Here, H-9 observation data are compared with reference values computed using radiation transfer codes from Aqua and Terra MODIS data.

Ray-matching approach w. NOAA-20/VIIRS

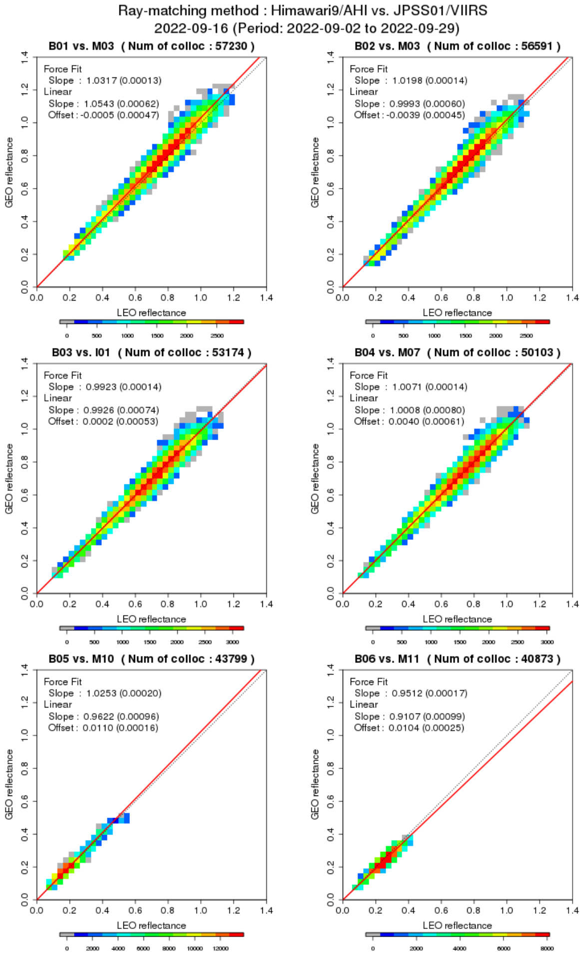

x-axis: reference based on VIIRS
y-axis: H-9/AHI observation

RTM based approach w. Aqua/MODIS

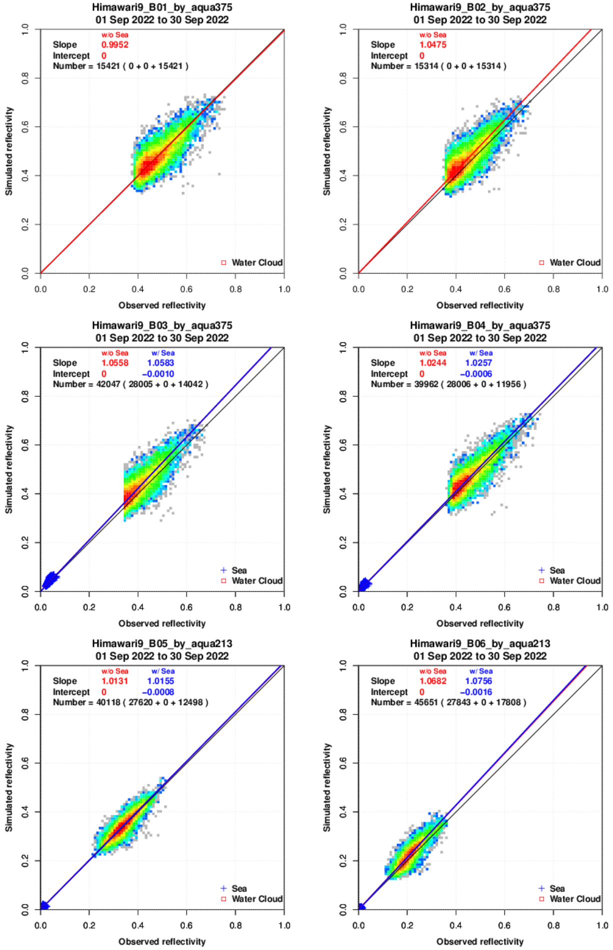

x-axis: H-9/AHI observation
y-axis: reference based on MODIS

II. Evaluation of calibration in consideration of SRF differences (B01 – B06)

Results

- H-8 and H-9 data are within around 5% of reference values, with differences depending on validation methods and imager references.
- Differences of 5 – 8% may be seen in reference data for B06. The correction coefficient will be set to the Himawari standard data.
- Rather than being direct comparisons between H-8 and H-9, these results represent biases from subtraction relating to SRF differences.

	H9AHI / reference				H8AHI / reference			
	RTM Aqua/MODIS	RTM Terra/MODIS	Ray-matching SNPP/VIIRS	Ray-matching N20/VIIRS	RTM Aqua/MODIS	RTM Terra/MODIS	Ray-matching SNPP/VIIRS	Ray-matching N20/VIIRS
B01	1.005	1.014	1.009	1.032	0.962	0.973	0.963	0.986
B02	0.955	0.965	0.998	1.020	0.951	0.961	0.991	1.014
B03	0.947	0.957	0.964	0.992	0.970	0.981	0.989	1.013
B04	0.976	0.989	0.972	1.007	0.979	0.993	0.974	1.010
B05	0.987	0.977	0.993	1.025	1.040	1.031	1.054	1.090
B06	0.936	0.922	0.926	0.951	0.946	0.931	0.941	0.967

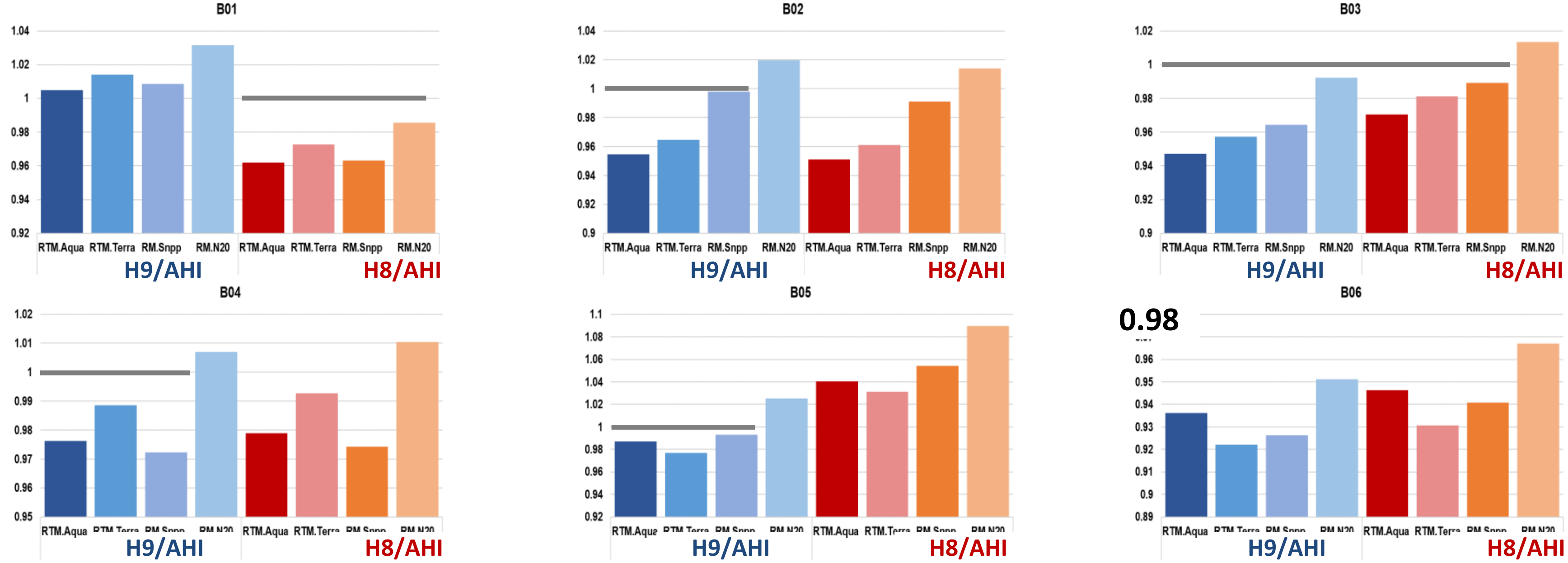

Data period:
RTM vicarious cal.: 1st – 30th Sep. 2022
Ray-matching: 2nd – 30th Sep. 2022

II. Evaluation of calibration in consideration of SRF differences (B01 – B06)

Trend

- The figures show evaluations of health-check observations carried out in 2017 and 2018 in addition to data from 2022.
- The trends potentially show sensitivity changes of 2 – 5% compared to 2017 health check observations. Further monitoring is necessary due to the short period of parallel observation for 2022 .

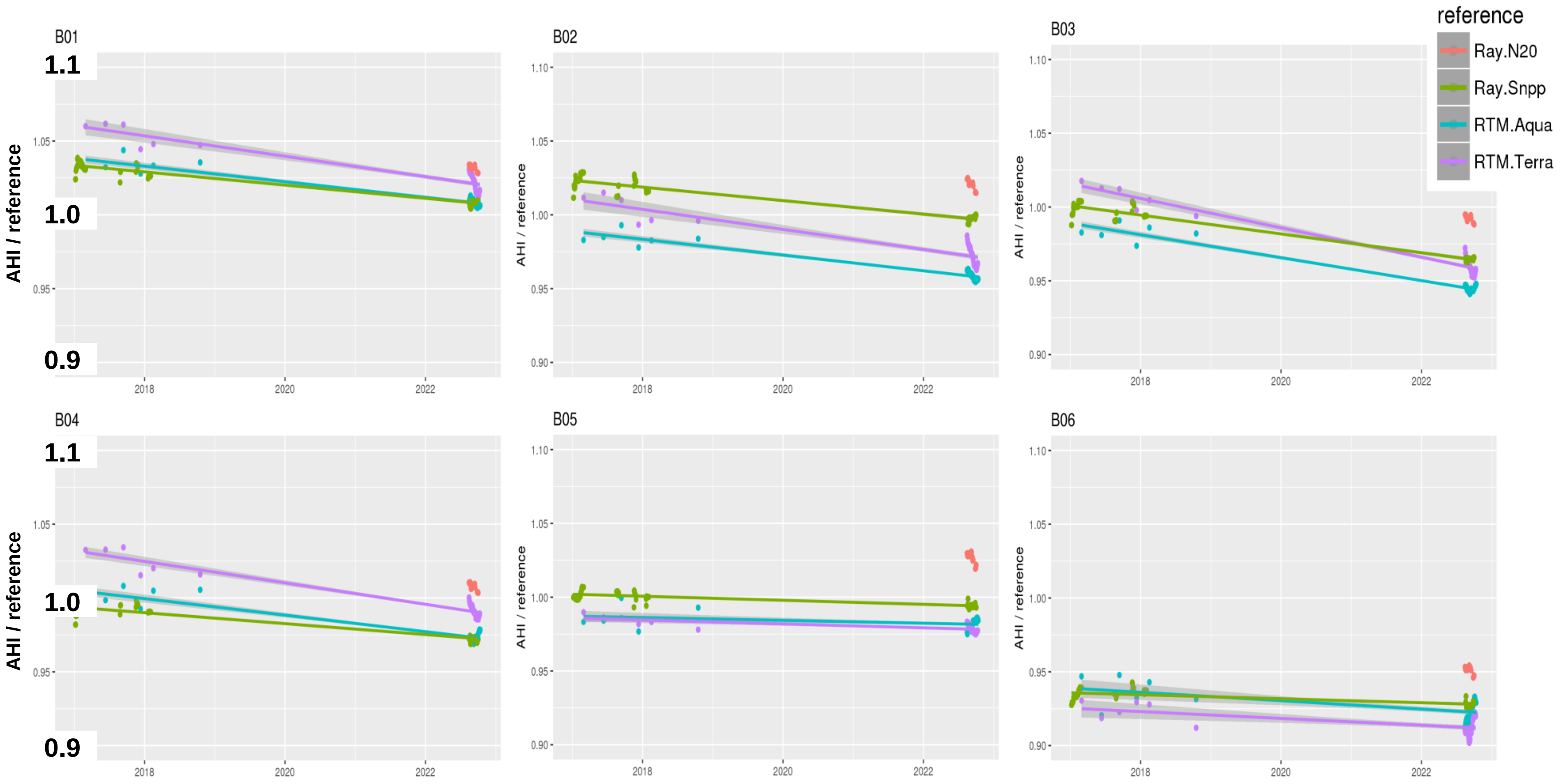

II. Evaluation of calibration in consideration of SRF differences (B07-B16)

Approach

- Based on infrared hyperspectral sounder observation (AIRS, CrIS, IASI), reference values are produced in consideration of AHI SRFs and compared with AHI observations for evaluation[4].
- Observation and reference values are linearly regressed based on radiance values (top) and evaluated as biases after conversion to brightness temperatures (bottom).
- Brightness temperature (Tb) bias generally depends on observed Tb. Bias values for clear sky sea surface temperature (standard radiance – the solid pink line in the lower figure) is shown in the following slides.
- Rather than being direct comparisons between H-8 and H-9, these results represent comparisons between AHI and reference values based on hyperspectral sounders.

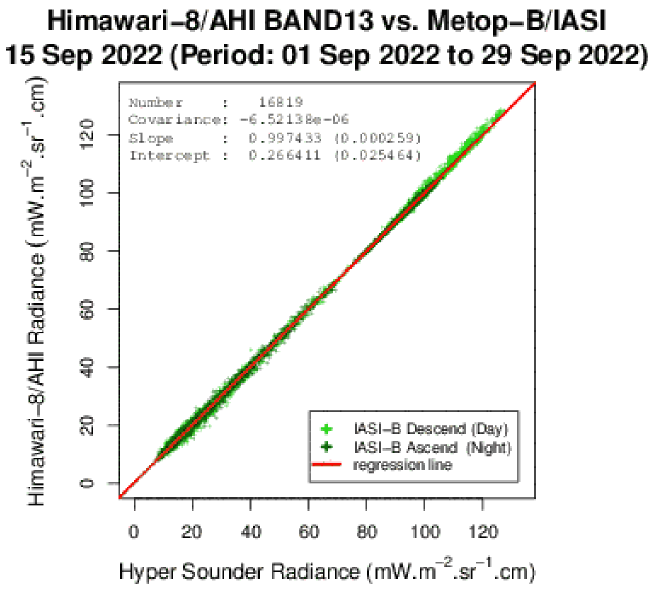

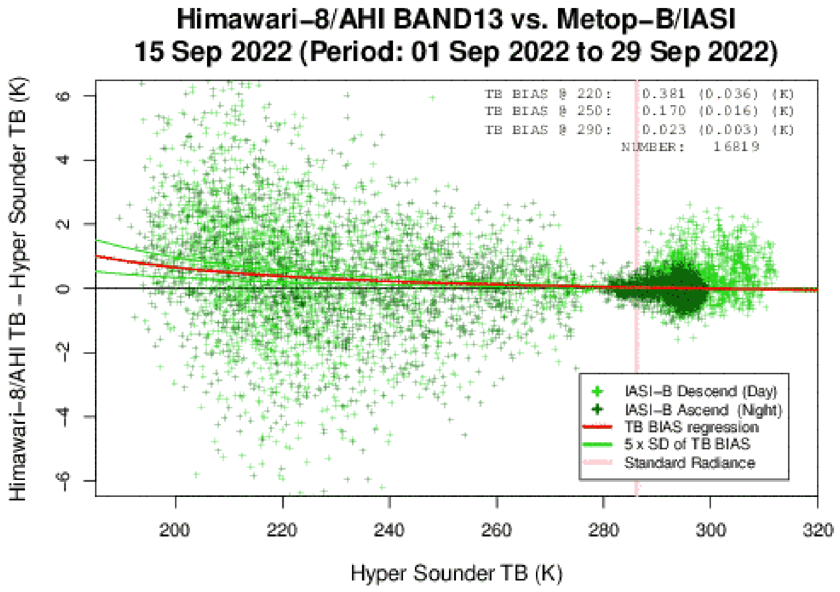

II. Evaluation of calibration in consideration of SRF differences (B07-B16)

Results

- Brightness temperature (Tb) biases for H-8 and H-9 are within 0.3 K at the standard radiance corresponding to clear-sky sea surface temperature.
- General stability is observed (see next slide).
- High values are observed at lower temperatures in some cases similar to H-8.

Tb bias at the standard radiance [K]
AHI wrt. Metop-B/IASI

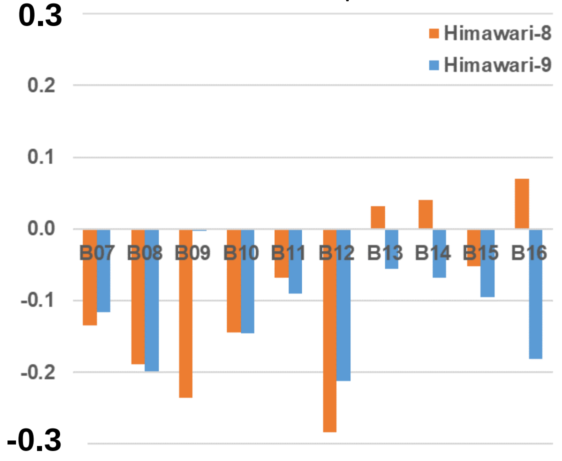

Tb bias at the standard radiance [K]

	H9/AHI – reference [K]				H8/AHI – reference [K]			
	Aqua/ AIRS	N20/CrIS	MetopB /IASI	MetopC /IASI	Aqua/ AIRS	N20/CrIS	MetopB /IASI	MetopC /IASI
B07	0.086	-	-0.116	-0.112	0.040	-	-0.134	-0.126
B08	-	-0.174	-0.199	-0.201	-	-0.164	-0.189	-0.193
B09	-0.087	0.029	-0.003	-0.002	-0.332	-0.208	-0.235	-0.234
B10	-0.204	-0.117	-0.145	-0.135	-0.218	-0.120	-0.144	-0.143
B11	-	-	-0.090	-0.080	-	-	-0.068	-0.057
B12	-0.196	-0.119	-0.212	-0.170	-0.249	-0.187	-0.284	-0.236
B13	-0.040	-0.017	-0.056	-0.052	0.063	0.073	0.032	0.038
B14	-0.047	-0.030	-0.068	-0.062	0.073	0.078	0.040	0.045
B15	-0.040	-0.058	-0.096	-0.086	0.010	-0.019	-0.053	-0.043
B16	-0.097	-0.148	-0.182	-0.166	0.149	0.098	0.070	0.086

Data period:
2^{nd} – 30^{th} Sep. 2022

- The bias wrt. CrIS at B07, the bias wrt. AIRS at B08 and the bias wrt. AIRS and CrIS at B11 are omitted because of its large uncertainty.
- See next slide for specific values of the standard radiances for each band.

II. Evaluation of calibration in consideration of SRF differences (B07-B16)

Trend

AHI9 wrt. Metop-B/IASI

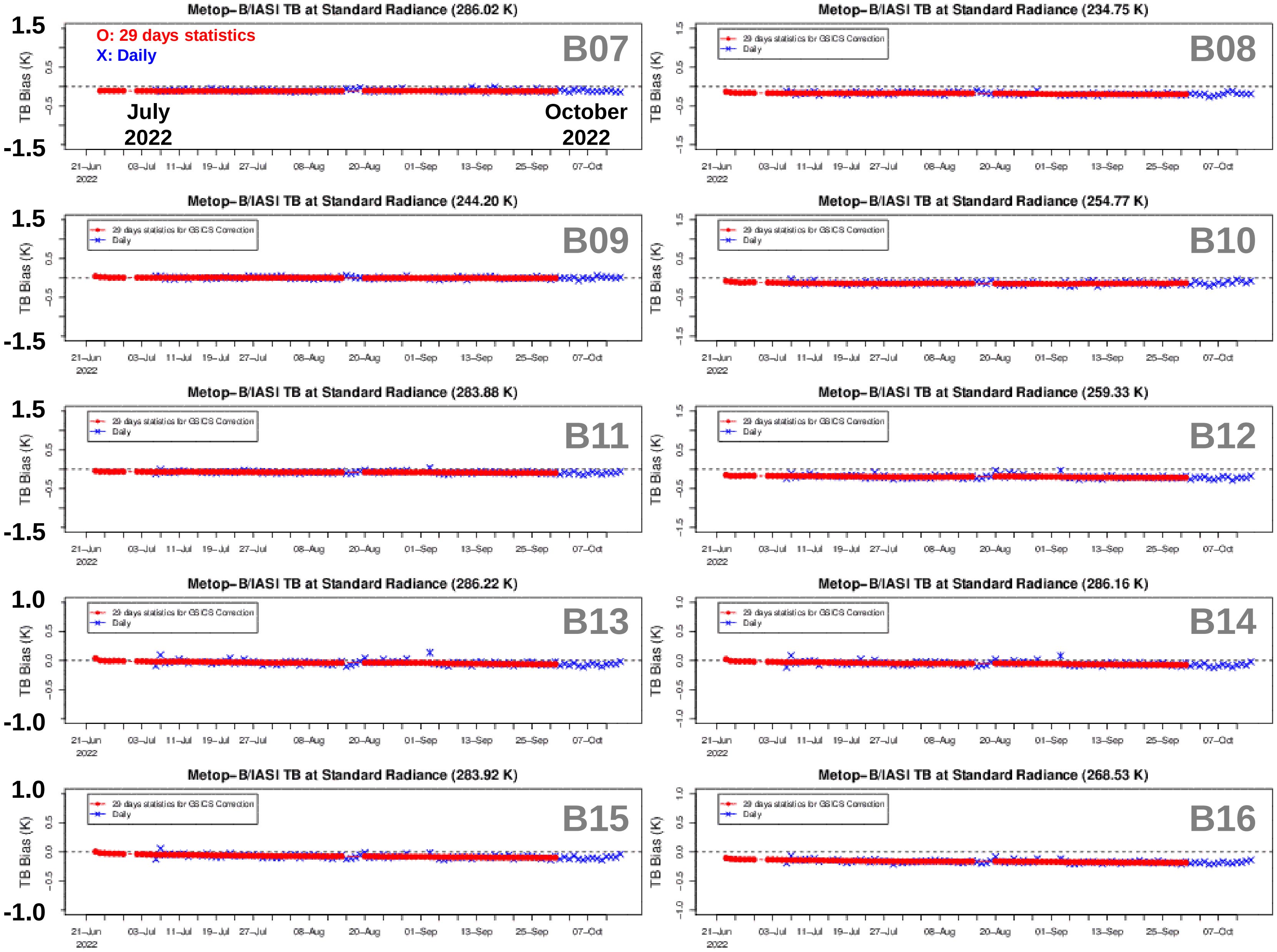

II. Evaluation of calibration in consideration of SRF differences (B07-B16)

Diurnal variation

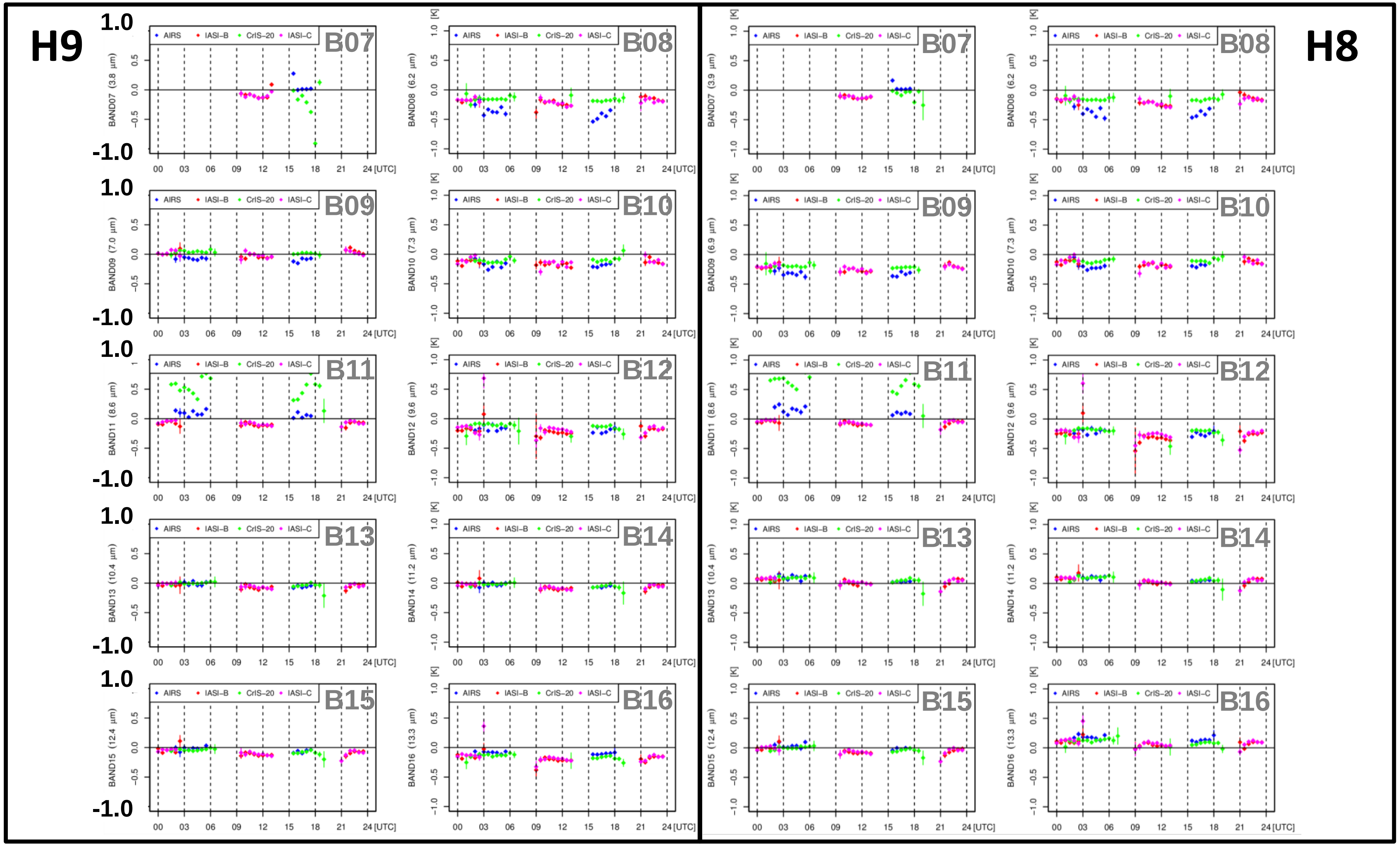

Data period:
2nd – 30th Sep. 2022

- Diurnal variations in Tb bias at the standard radiance (x-axes show time in UTC) are shown.
- No significant variations are observed.
- Significant uncertainty is seen in the bias wrt. CrIS at B07, AIRS at B08, and AIRS and CrIS at B11.

other topic: OFAR (Out of Field Anomalous Response)

- OFAR[5] is observed only in extremely high-contrast environments such as outer space and the lunar surface.
- OFAR is observed only in B01, B02 and B03.
- There are no effects in Earth observation.
- OFAR is observed to the same extent for H-8 and H-9.

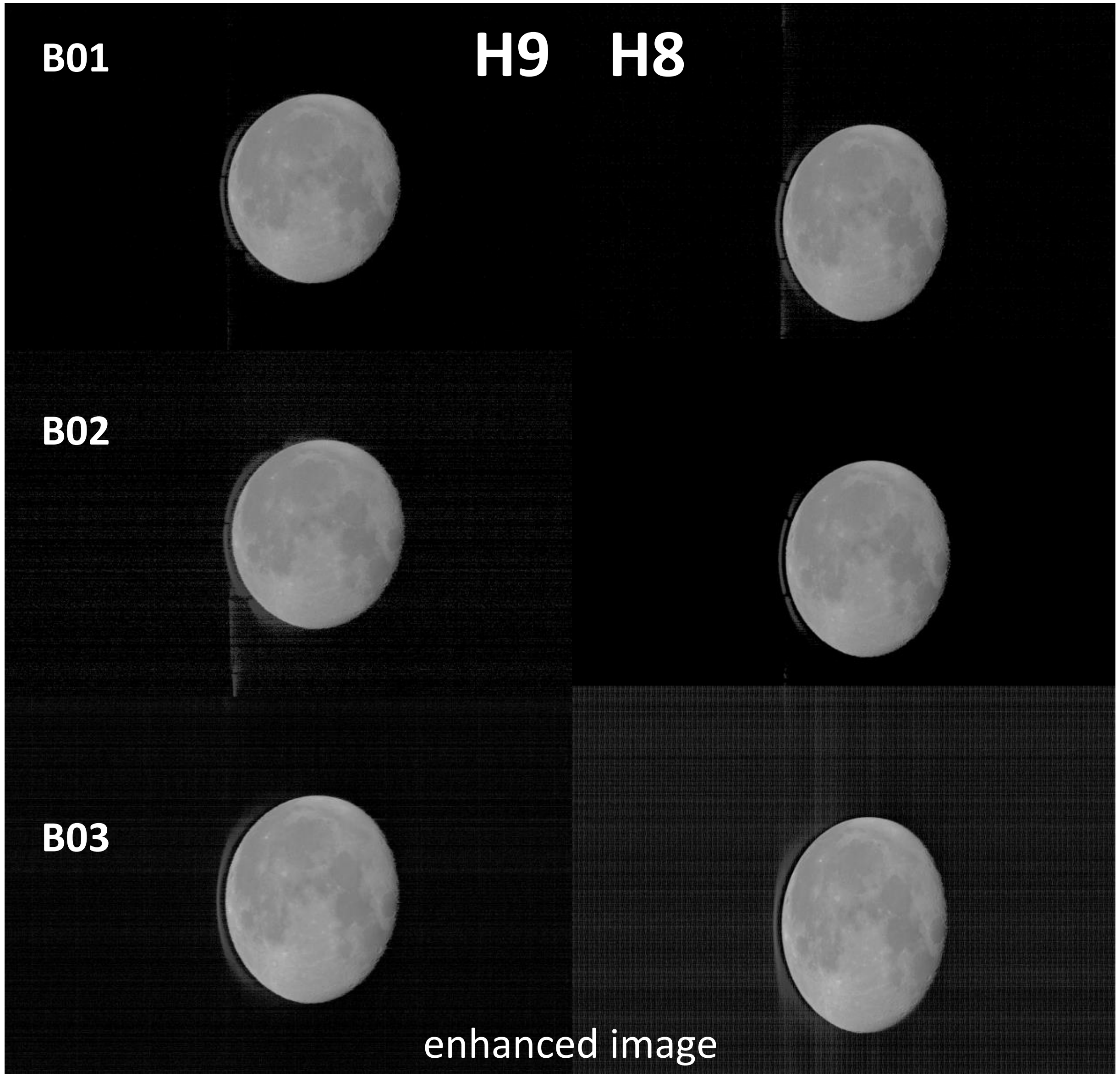

Summary

- Navigation accuracy
  - Absolute accuracy based on landmark analysis and band-to-band registration accuracy are generally the same as for H-8.
- Calibration evaluation in VIS/NIR bands
  - Differences from H-8 data are within 5%.
  - Differences from reference values are within 5% for B01 to B05 and 5 – 8% for B06 based on MODIS and VIIRS. JMA plans to set correction coefficients in Himawari standard data a year later in consideration of seasonal variations.
- Calibration evaluation in infrared bands
  - Differences are within 0.3 K of H-8 data.
  - Differences from references are within 0.3 K based on data from infrared hyperspectral sounders on LEO satellites.
  - The magnitude of diurnal change is similar to that of H-8.

References

[1] Doelling D., R. Bhatt, D. Morstad, B. Scarino, "Algorithm Theoretical Basis Document (ATBD) for ray-matching technique of calibrating GEO sensors with Aqua-MODIS for GSICS", 2011, http://gsics.atmos.umd.edu/pub/Development/AtbdCentral/GSICS_ATBD_RayMatch_NASA_2011_09.pdf (Accessed: 06 November 2022)

[2] B. R. Scarino, D. R. Doelling, P. Minnis, A. Gopalan, T. Chee, R. Bhatt, C. Lukashin, and C. O. Haney, "A web-based tool for calculating spectral band difference adjustment factors derived from SCIAMACHY hyperspectral data", IEEE Trans. Geosci. Remote Sens., vol. 54, no. 5, pp. 2529-2542, 2016.

[3] A. OKUYAMA, M. TAKAHASHI, K. DATE, K. HOSAKA, H. MURATA, T. TABATA, and R. YOSHINO, "Validation of Himawari-8/AHI Radiometric Calibration Based on Two Years of In-Orbit Data", J. of the Met. Soc. of Japan, vol. 96B, pp. 91–109, 2018

[4] Hewison, T. J., X. Wu, F. Yu, Y. Tahara, X. Hu, D. Kim and M. Koenig, "GSICS Inter-Calibration of Infrared Channels of Geostationary Imagers Using Metop/IASI", IEEE Trans. Geosci. Remote Sens., vol. 51, no. 3, pp. 1160-1170, 2013

[5] Paul C. Griffith and David S. Smith, "HIMAWARI-8 OUT-OF-FIELD ANOMALOUS RESPONSE (OFAR)", 8th Asia/Oceania Meteorological Satellite Users' Conference, 18-20 October 2017, Vladivostok, Russian Federation